Mercury Binding on Activated Carbon

Bihter Padak, Michael Brunetti, Amanda Lewis, and Jennifer Wilcox
Department of Chemical Engineering, Worcester Polytechnic Institute, Worcester, MA 01609; jwilcox@wpi.edu (for correspondence)

Published online 2 November 2006 in Wiley InterScience (www.interscience.wiley.com). DOI 10.1002/ep.10165

Density functional theory has been employed for the modeling of activated carbon (AC) using a fused-benzene ring cluster approach. Oxygen functional groups have been investigated for their promotion of effective elemental mercury binding on AC surface sites. Lactone and carbonyl functional groups yield the highest mercury binding energies. Further, the addition of halogen atoms has been considered to the modeled surface, and has been found to increase the AC's mercury adsorption capacity. The mercury binding energies increase with the addition of the following halogen atoms, F > Cl > Br > I, with the fluorine addition being the most promising halogen for increasing mercury adsorption. © 2006 American Institute of Chemical Engineers Environ Prog, 25: 319–326, 2006

Keywords: mercury capture, activated carbon, halogen, density functional theory, adsorption

INTRODUCTION

Emissions from coal combustion processes constitute a significant amount of the elemental mercury released into the atmosphere today. Coal-fired power plants are the greatest anthropogenic source of mercury emissions in the United States [1]. Reducing the emissions of mercury is a major environmental concern since mercury is considered to be one of the most toxic metals found in the environment [2] and additionally is considered a hazardous air pollutant (HAP) by The Clean Air Act (CAA) of 1990. Mercury released into the environment can precipitate into lakes, rivers, and estuaries and can be converted through biological processes into an organic form, methylmercury, which is a neurotoxin that bioaccumulates in fish, animals, and mammals [3,4]. Mercury has adverse effects on the central nervous system and causes pulmonary and renal failure, severe respiratory damage, blindness, and chromosome damage [5,6]. In March 2005, EPA adopted the Clean Air Mercury Rule to reduce mercury emissions from coal-fired power plants, [1] which will ultimately reduce the US emissions of mercury to 15 tons a year, constituting an approximate 70% reduction.

Mercury exists in coal combustion flue gas in a variety of forms depending on the coal type and combustion conditions; i.e., elemental (Hg^0), oxidized ($HgCl_2$ or HgO), and particulate ($Hg_{(p)}$). Most of the mercury particulates, which comprise 10% of the total mercury in the flue gas can be removed using air pollution control devices. Oxidized mercury, i.e. Hg^{+2}, is easily captured by wet scrubbers, while gaseous elemental mercury passes through the scrubbers readily. It is difficult to capture elemental mercury because of its insolubility in water, higher volatility, and chemical inertness [7]. Particulate matter such as fly ash, unburned carbon, and activated carbon (AC) can be used to capture elemental and oxidized mercury through adsorption processes. Interaction of gaseous mercury with particulate matter can either lead to adsorbed and subsequent retained mercury on the surface, or can serve to oxidize elemental mercury to a water-soluble form for capture in wet scrubbers.

Many studies have been performed to find an effective and affordable sorbent for the removal of elemental mercury from combustion flue gas. AC is one of the most studied sorbents for capturing mercury. AC adsorption can be performed through two different processes, i.e., powdered activated carbon (PAC) injection or fixed-bed granular activated carbon (GAC) adsorption. The use of PAC involves the direct injection of AC into the plant's flue gas stream where it adsorbs gaseous mercury and is collected in downstream particulate control devices, such as fabric filters or electrostatic precipitators (ESP). In the case of using GAC, an adsorber is placed downstream of the flue gas desulfurization (FGD) unit along with particulate collectors, which serve as the final treatment process before the flue gas is discharged into the atmosphere [8].

It has been shown that chemically embedded activated carbon has a higher mercury adsorption capacity than thermally AC. Specifically, sulfur-, chlorine-, bromine- and iodine-embedded AC have been found to be effective sorbents for elemental mercury capture. It has been observed that at 150–260°C, AC embedded with chlorine salt has as much as a 300 times greater elemental mercury removal capacity than traditional thermally AC [9]. It has also been reported by Matsumura [10] that oxidized or iodized AC adsorbed mercury vapor 20–160 times more than untreated AC in nitrogen at 30°C. Granite *et al.* [11] stated that hydrochloric acid-treated AC yielded a large capacity of mercury in the experiments carries out in argon at 138°C, which makes it one of the most active sorbents studied to date. However, the cost related to the preparation of chemically embedded AC is high. There have been many attempts to find a low-cost alternative sorbent, but limited success has resulted due to problems associated with removal efficiency [12]. Therefore, it is essential to develop a novel sorbent for the effective and affordable removal of elemental mercury.

Krishnan *et al.* have shown that the type of AC, reaction temperature and inlet Hg^0 concentration affect adsorption rates and capacity for elemental mercury. They have found elemental mercury sorption on thermally AC to be decreasing with increasing temperature [12]. It has been illustrated by many studies that adsorption process of mercury on AC surface is exothermic, indicating a typical physisorption mechanism [12–16]. Moreover, sulfur, iodine and chlorine impregnants are thought to provide sites where the mercury can chemically adsorb onto the carbon surface [17]. For chlorine and sulfur impregnated ACs the lower the temperature the higher the adsorption capacity of mercury because of exothermic behavior of mercury reaction with chloride [17–20] or elemental sulfur [21,8]. Conversely, in the case of iodine impregnated AC the amount of mercury adsorbed by the carbon increases as the temperature increases [22].

Studies performed at Energy & Environmental Research Center (EERC) have examined the effects of flue gas acid species such as HCl, SO_2, NO, NO_2 on mercury capture as well as mercury binding and oxidation mechanism. In the model they have proposed, electrons must be accepted by a Lewis acid on AC and then Hg^{+2} which is a Lewis acid can bind to Lewis base sites on the surface competing with other acidic species i.e., HCl and sulfuric acid [23–26].

Investigations carried out by Carey *et al.* [27] have found that the type of carbon sorbent and its associated chemical properties are the most important factors affecting elemental mercury adsorption for a given flue gas composition. It has been observed that moisture within the AC matrix plays an important role in promoting elemental mercury adsorption at room temperature [28]. Lee and Park [29] observed that virgin AC with large oxygen functional groups was superior in mercury adsorption performance. Li *et al.* [30] also studied the effect of AC's oxygen surface functional groups such as lactone, carbonyl, phenol, and carboxyl on elemental mercury adsorption. They found that both lactone and carbonyl groups are the likely active sites for mercury adsorption on an AC surface. They also investigated whether phenol groups may inhibit mercury adsorption and whether the AC surfaces having a lower phenol to carbonyl ratio yield a greater elemental mercury adsorption capacity.

Table 1. C—Cl bond distances (Å) for different positions of Cl_2.

	Armchair edge	Zigzag edge	Center
C—Cl	1.8137	1.8258	4.5093

Not only have experimental studies been performed in this area, but theoretical studies have also been carried out to gain an increased understanding of the mechanisms involved in elemental mercury adsorption onto AC surfaces. To the authors' knowledge this is the first *ab initio*-based investigation involving the adsorption of elemental mercury on halogen-embedded AC thus far. However, there have been theoretical investigations involving adsorption on graphite, which have provided ideas on how to begin modeling a carbon surface.

Chen and Yang [31,32] have investigated different theoretical methods and different graphite models for describing graphite surface using *ab initio* methods. Comparing geometry, frequency, and bond parameters calculated at different levels of theory to the experiment, B3LYP/6-31G(d)//HF/3-21G(d) has been found to be the most accurate and cost-effective method. Six graphite models with increasing sizes from 1 to 7 with seven fused benzene rings were considered at the chosen level of theory. According to their comparison, $C_{25}H_9$ is the most suitable model among the others representing a single layer graphite surface.

Lamoen and Persson [33] have performed a study on the adsorption of potassium (K) and oxygen on graphite surfaces based on the Monte Carlo simulations. They have used a periodically repeated hexagonal supercell of n graphite layers ($n = 1,2,3$) and showed that the main physics is correctly described by a single graphite layer. Zhu and Lu [34] compared the adsorption of alkali metals on graphite surfaces modeled as 7, 10, 12, and 14-fused benzene rings. Since Janiak *et al.* [35] and Lamoen and Persson [33] have found that the difference of K adsorption on single-layer graphite and multilayer graphite is negligible, they chose single-layer graphite for their studies. Investigating three different sites for adsorption they showed that the "middle hollow site" above a hexagon is the most stable position for the adsorptions of Li, K, and Na. Their analysis indicated that, comparing two levels of theory, the results from MP2 are not as reliable as those from B3LYP. The binding energies obtained at B3LYP/6-31G(d,p) are in good agreement with other theoretical studies.

Ohta and Ohta [36] investigated the adsorption of hydrogen on graphite using B3LYP/6-31G(d) level of theory. Pyrene, which has four closely fused aromatic rings ($C_{16}H_{10}$) was used in the calculations for simulating graphite surface. Pliego *et al.* [37] studied the chemisorption of SO_2 on a graphite surface investigating the adsorption sites as well as the stability of the adsorbed

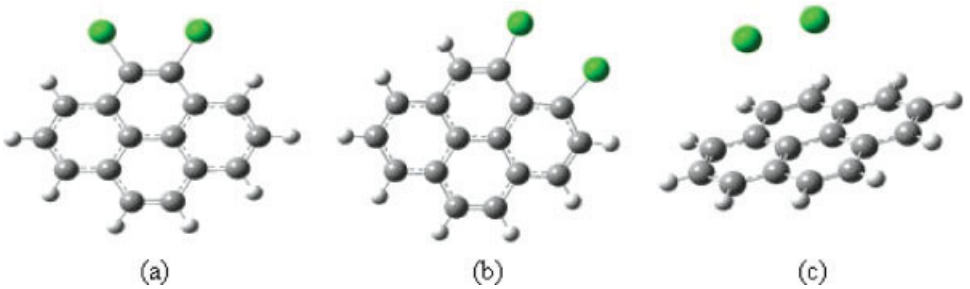

Figure 1. Optimized geometries for Cl_2 on different sites of the cluster (a) armchair edge; (b) zigzag edge; (c) center. [Color figure can be viewed in the online issue, which is available at www.interscience.wiley.com.]

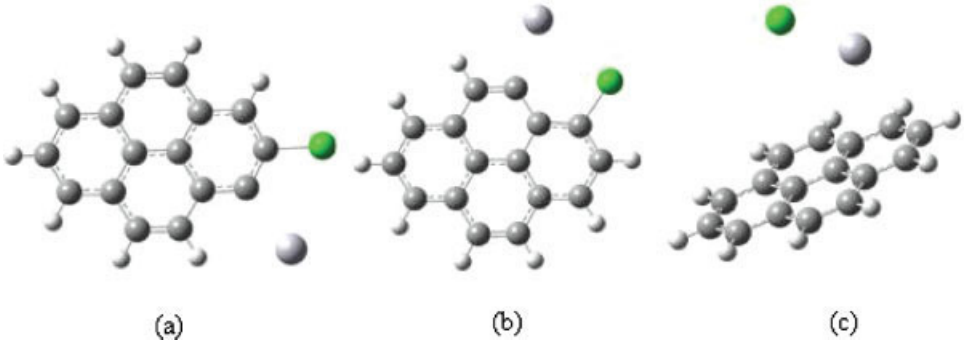

Figure 2. Optimized geometries for Hg and Cl on different sites of the cluster (a) armchair edge; (b) zigzag edge; (c) center. [Color figure can be viewed in the online issue, which is available at www.interscience.wiley.com.]

Table 2. C—Cl and C—Hg bond distances (Å) for different positions on the surface.

	Armchair edge	Zigzag edge	Center
C—Cl	1.8461	1.8345	5.7448
C—Hg	2.4613	2.4788	4.0836

complexes. HF/6-31G(d) level of theory was utilized in the geometry optimization. Frequency and single-point calculations were performed at MP2/6-31G(d) to obtain reaction energies. The pyrene structure and two dehydrogenated derivatives corresponding to armchair and zigzag edges were used in modeling the graphite surfaces to simulate different adsorption sites. They have found adsorption to be favorable on an arm chair edge with binding energies of −5 to −51 kcal/mol and found adsorption on a zigzag edge to be the most favorable with binding energies ranging from −61 to −100 kcal/mol.

Collignon *et al.* [38] used *ab initio* methods to understand the mechanism associated with water adsorption on hydroxylated graphite surfaces. The graphite surface consisted of 30-fused benzene rings ($C_{80}H_{22}$), which represents a nanometer-size graphite crystallite. To optimize such a large surface, the two layers ONIOM method was utilized, which divides the system into two nested regions. These regions are considered with different model chemistries and then merged into the final predicted results. The central part of the system that contains the water molecules, the OH group and the closest neighboring C and H atoms is modeled with B3LYP method while the rest of the system is modeled with the semiempirical PM3 method so that a balance between accuracy and computational time has been obtained. All of these previous studies have focused on understanding the structure of AC and its active sites and the role they play in adsorption mechanisms. Limited theoretical investigations have been performed on the mechanism responsible for the adsorption of mercury on AC surfaces.

Steckel [39] has investigated the interactions between elemental mercury and a single benzene ring, which is quite limited in its potential for representing an accurate carbon surface. However, this previous study is the first to begin the investigations required for elucidating the mechanism by which elemental mercury binds to carbon. No known research has been conducted toward understanding the mechanism of mercury adsorption on simulated halogen-embedded AC surfaces. The objective of the current study is applying theoretical-based cluster modeling to examine the effects of AC's different surface functional groups and halogens on elemental mercury adsorption. This research will provide direction for further experimental studies that will aid in the development of a novel sorbent for effective mercury capture.

COMPUTATIONAL METHODOLOGY

The Gaussian03 software package [40] was used for all of the energetic predictions in this work. Density Functional Theory (DFT) was employed due to its sim-

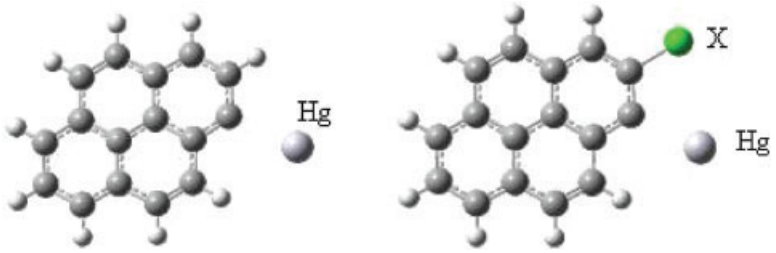

Figure 3. Cluster models of mercury adsorbed on activated carbon (AC) and halogen-embedded activated carbon. X: F, Cl, Br, I. [Color figure can be viewed in the online issue, which is available at www.interscience.wiley. com.]

Table 3. Mercury binding energies (kcal/mol) and C—X bond distances associated with the clusters from Figure 2.

	Binding energies (kcal/mol)	C—X Bond distances (Å)
AC	−4.3235	–
AC—F	−9.5885	1.4178
AC—Cl	−7.7207	1.8461
AC—Br	−6.6431	1.9809
AC—I	−5.3697	2.1681

plicity and accuracy. Considering that mercury has eighty electrons, to account for relativistic effects, a basis set with the inner electrons substituted by effective core potentials (ECP) was chosen. Beck's three-parameter functional with a Lee-Yang-Parr gradient-corrected correlation functional (B3LYP) with LANL2DZ basis set which uses an all-electron description for the first-row elements and an ECP for inner electrons and double-ζ quality valence functions for the heavier elements was used for the energy predictions [41–43].

RESULTS AND DISCUSSION

Modeling Activated Carbon Surface

For the theoretical model it was assumed that the activated carbon (AC) molecular framework is similar to that of graphite. Pyrene was examined to serve as a representative cluster species to model the AC surface. A larger cluster, possibly more accurate, would require greater computational effort. Through comparing the structure predictions of four- and seven-fused benzene rings, the four-fused rings were chosen since the calculations provide a reasonable balance between accuracy and computational expense.

To optimize a halogen-embedded AC surface, halogens were embedded at different sites along the cluster surface, i.e. the armchair edge, zigzag edge and center site. Optimization calculations have been carried out using the B3LYP method with the LANL2DZ basis set. The optimized bond distances of carbon and chlorine atoms are presented in Table1 with the optimized structures shown in Figure 1. The theoretical geometry predictions convey that there is a minimal difference between the C—Cl bond distance from either the armchair or zigzag edge sites, while this bond distance is much greater at the center site. More calculations have been performed using a bromine-embedded surface at the HF/SDD and HF/6-311G levels of theory and similar results have been obtained. It has been noted that no stable complex can be formed when halogens are embedded at the center of the cluster.

Table 4. C—Hg bond distances (Å) for the clusters associated with the clusters from Figure 3.

	Lactone	Carbonyl	Phenol	Carboxyl
C—Hg	2.4462	2.2586	2.4497	2.5078

Moreover, a single Hg atom and a Cl atom have been optimized at different sites on the surface and the optimized geometries are shown in Figure 2 while the bond distances are given in Table2. The same trend has been observed, i.e. that no stable complex can be formed at the center site and therefore, edge sites were chosen to be used in the further calculations. Also, comparison of mercury binding energies for zigzag and armchair edge sites shows that the armchair edge is more favorable for mercury binding with a binding energy of 7.72 kcal/mol while zigzag edge has a binding energy of 3.5 kcal/mol.

Effect of Halogens on Hg Adsorption Capacity

Previous experimental studies have shown that chemically embedded AC has a higher elemental mercury removal capacity than thermally AC. In particular, halogen-embedded AC has been found to be an effective sorbent for elemental mercury capture [9–12,44]. To understand the interactions between elemental mercury and halogen-embedded AC, density functional theory calculations have been performed using different halogens such as fluorine, chlorine, bromine, and iodine. The AC cluster having mercury and halogen at the armchair edge has been modeled at the B3LYP/LANL2DZ level of theory. Cluster models with and without halogens are shown in Figure 3. Binding energies of elemental mercury on the AC clusters were calculated using Eq. 1:

$$\text{Binding Energy} = \text{E(AC} - \text{Hg)} - [\text{E(Hg)} + \text{E(AC)}] \qquad (1)$$

Comparing the binding energies of elemental mercury on the AC surface with and without a halogen indicates that the use of a halogen promotes mercury

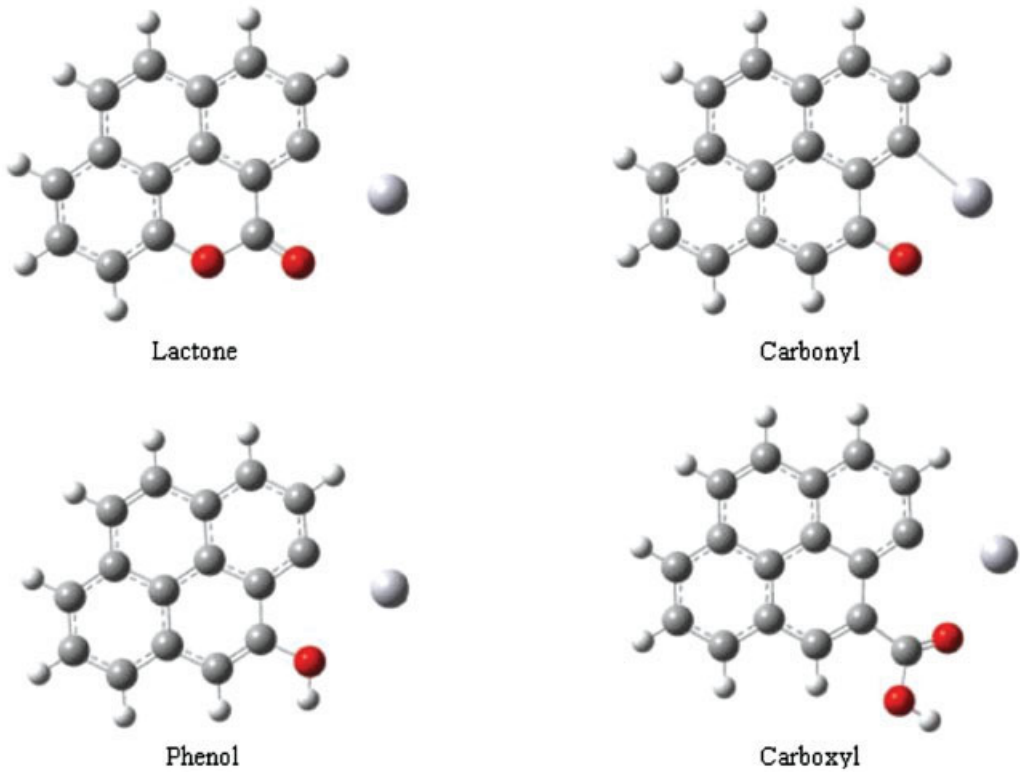

Figure 4. Activated carbon clusters with oxygen functional groups: lactone, carbonyl, phenol, and carboxyl. [Color figure can be viewed in the online issue, which is available at www.interscience.wiley.com.]

binding. Examination of the binding energies reported in Table3 reveals that fluorine yields the highest binding energy, i.e. −9.59 kcal/mol, compared to the other halogens considered.

Effect of Oxygen Functional Groups on Hg Adsorption Capacity

Experimental studies conducted by Lee and Park [29] indicate that AC with large oxygen functional groups were superior for elemental mercury adsorption. To simulate an AC surface with increased accuracy, oxygen functional groups such as carbonyl, lactone, carboxyl, and phenol groups were also considered on the cluster. Each functional group has been investigated separately to note the effect of different functional groups on elemental mercury binding. Carbon-mercury bond distances for the optimized clusters are given in Table4, with the optimized structures presented in Figure 4.

Lactone and carbonyl groups have been found to be active sites for mercury binding, yielding binding energies of −10.29 and −9.16 kcal/mol, respectively. The presence of phenol and carboxyl groups has yielded relatively lower binding energies, −6.72 and −1.22 kcal/mol, respectively. More specifically, the presence of lactone and carbonyl functional groups promotes the chemisorption of elemental mercury while phenol and carboxyl functional groups promote a physisorption mechanism of mercury adsorption. These results agree with the experimental results of Li *et al.* [30] where they found both lactone and carbonyl groups to be the likely sites for mercury adsorption, with the AC surfaces having a lower phenol to carbonyl ratio yielding a greater elemental mercury adsorption capacity.

Since it is known that halogen-embedded AC has higher elemental mercury adsorption capacities than traditional AC, halogens combined with the oxygen functional groups have been considered. Halogen-embedded clusters with different oxygen functional groups have been investigated and are shown in Figure 5. For these clusters the bond distances of carbon-halogen and carbon-mercury are given in Table5. The binding energies reported in Table6 show that adding a halogen to the cluster increases the elemental mercury adsorption capacity. It is interesting to note that the mercury binding energy increases with decreasing halogen distance to the AC cluster surface as it is seen from Table 3. Further investigations would be required to determine whether the halogen proximity directly influences the activity of the binding sites.

Using different halogens with surface functional groups, the same trend has been observed where fluorine yields the highest binding energy of elemental mercury. The best binding performance has been obtained with the fluorine atom and lactone functional group combination, which has a mercury binding energy of −16.71 kcal/mol, while the second best is a carbonyl functional group with fluorine atom having a binding energy of −14.5 kcal/mol. Although the phenol functional group does not yield a promising adsorption capacity, when fluorine is used, it may exist as an active site for elemental mercury adsorption.

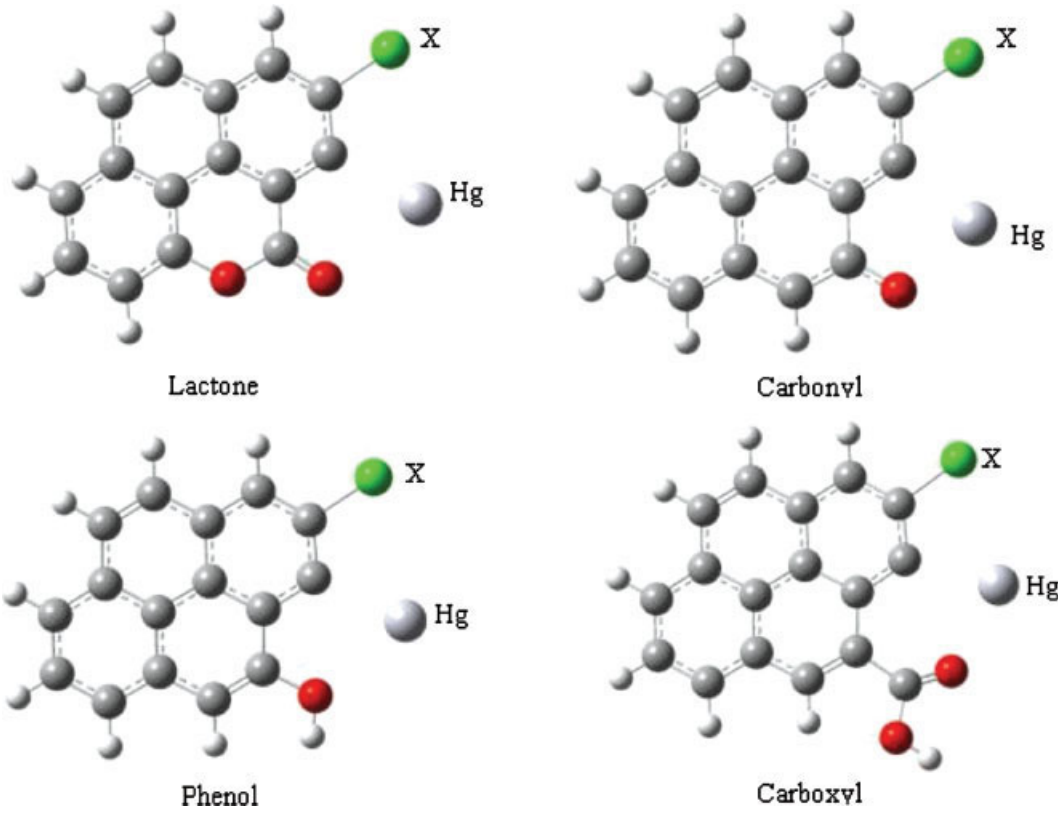

Figure 5. Halogen-embedded activated carbon clusters with oxygen functional groups: lactone, carbonyl, phenol, and carboxyl. X = F, Cl, Br, I. [Color figure can be viewed in the online issue, which is available at www.interscience.wiley.com.]

Table 5. Bond distances (Å) of the clusters represented in Figure 4.

Functional groups	X=F		X=Cl		X=Br		X=I	
	C—Hg	C—F	C—Hg	C—Cl	C—Hg	C—Br	C—Hg	C—I
Lactone	2.4096	1.4116	2.4239	1.8395	2.4307	1.9891	2.4382	2.1640
Carbonyl	2.2608	1.4096	2.2671	1.8336	2.2678	1.9809	2.2730	2.1525
Phenol	2.3954	1.4165	2.4150	1.8468	2.4254	1.9959	2.4314	2.1718
Carboxyl	2.4428	1.4220	2.4616	1.8564	2.4690	2.0069	2.4747	2.1824

Table 6. Binding energies of mercury on halogen-embedded activated carbon with different oxygen functional groups: lactone, carbonyl, phenol, and carboxyl.

Functional groups	Binding energies (kcal/mol)				
	AC	AC—F	AC—Cl	AC—Br	AC—I
Lactone	−10.2851	−16.7144	−14.6622	−13.4594	−11.8763
Carbonyl	−8.8298	−14.5008	−13.0570	−12.1202	−10.9199
Phenol	−6.7242	−12.6310	−10.5091	−9.2009	−7.7716
Carboxyl	−1.2231	−7.6798	−4.0432	−2.4707	−0.6746

CONCLUSIONS

Note that these calculations do not represent real flue gas conditions and the calculated mercury binding energies have yet to be compared directly to experiment since such specific data is currently lacking in the literature. Effects of other flue gas constituents have not been considered and the simulations have been performed at room temperature. Density functional theory calculations have been carried out to provide a possible mechanism associated with mer-

cury binding on various types of AC. These results can provide a direction for further experiments in terms of through the recognition of binding trends and how the binding capacity changes by modifying the surface. In light of these results, AC with the best combination of halogen and oxygen surface functional groups yielding the highest mercury removal capacity can be used in the experiments.

Through comparing the binding energies of elemental mercury on simulated activated carbon surfaces, it can be concluded that increasing the amount of lactone and carbonyl groups and decreasing carboxyl group can increase the binding capacity of elemental mercury. In addition, embedding halogen, especially fluorine, into the activated carbon matrix, can possibly promote elemental mercury binding.

ACKNOWLEDGEMENT

This work was supported by the U.S. Environmental Protection Agency (Cooperative Agreements CR-83291001-0).

Disclaimer

This report has not been subject to review by this agency and therefore does not necessarily reflect their views and no official endorsement should be inferred.

LITERATURE CITED

1. U.S. Environmental Protection Agency. Fact sheet: EPA's clean air mercury rule, Washington, DC. (2005).
2. Clarkson, T.W. (1993). Mercury: Major issues in environmental health, Environmental Health Perspectives, 100, 31–38.
3. Sorensen, J.G., Glass, G.E., Schmidt, K.W., Huber, J.K., & Rapp, G.R. (1990). Airborne mercury deposition and watershed characteristics in relation to mercury concentrations in water, sediments, plankton, and fish of eighty Northern Minnesota lakes, Environmental Science & Technology, 24, 1716–1727.
4. Fitzgerald, W.F., Engstrom, D.R., Mason, R.P., & Nater, E.A. (1998). The case for atmospheric mercury contamination in remote areas, Environmental Science & Technology, 32, 1–7.
5. Berglund, F., & Bertin, M. (Eds.) (1969). Chemical fallout, Springfield, IL: Thomas.
6. WHO. (1990). Methylmercury, Environmental health criteria 101, World Health Organization, Geneva, (pp. 68–102).
7. Change, R., & Offen, G.R. (1995). Mercury emission control technologies: An epri synopsis, Power Engineering, 99, 51–57.
8. Korpiel, J.A., & Vidic, R.D. (1997). Effect of sulfur impregnation method on activated carbon uptake of gas-phase mercury, Environmental Science & Technology, 31, 2319–2325.
9. Teller, A.J., & Quimby, J.M. Mercury removal from incineration flue gas, Proceedings of the 84th Annual Meeting and Exhibition, AWMA, Vancouver, BC, (1991). 95, 35.5.
10. Matsumura, Y. (1974). Adsorption of mercury vapor on the surface of activated carbons modified by oxidation or iodization, Atmospheric Environment, 8, 1321–1327.
11. Granite, E.J., Pennline, H.W., & Hargis, R.A. (2000). Novel sorbents for mercury removal from flue gas, Industrial & Engineering Chemistry Research, 39, 1020–1029.
12. Krishnan, S.V., Gullett, B.K., & Jozewicz, W. (1994). Sorption of elemental mercury by activated carbons, Environmental Science & Technology, 28, 1506–1512.
13. Karatza, D., Lancia, A., Musmarra, D., & Zucchini, C. (2000). Study of mercury absorption and desorption on sulfur impregnated carbon, Experimental Thermal & Fluid Science, 21, 150–155.
14. Ghorishi, B., & Gullett, B.K. (1998). Sorption of mercury species by activated carbons and calcium-based sorbents: Effect of temperature, mercury concentration and acid gases, Waste Management & Research, 16, 582–593. (karatza 6 ghorishi gullet).
15. Gullett, B.K., & Jozewicz, W. (1993). NAME international conference on municipal waste combustion, Williamsburg, VA. (Krishnan 13 gullet jozevicz).
16. Zeng, H., Jin, F., & Guo, J. (2004). Removal of elemental mercury from coal combustion flue gas by chloride-impregnated activated carbon, Fuel, 83, 143–146.
17. Vidic, R.D., & Siler, D.P. (2001). Vapor-phase elemental mercury adsorption by activated carbon impregnated with chloride and chelating agents, Carbon, 39, 3–14.
18. Van Wylen, G.J., Sonntag, R.E., & Borgnakke, C. (1994). Fundamentals of classical thermodynamics (4th Edition), New York: Wiley. pp. 555–646.
19. Smith, J.M., & Van Ness, H.C. (1987). Introduction to chemical engineering thermodynamics (4th Edition, pp. 105–133), New York: McGraw-Hill.
20. Chase, M.W., Jr., Davies, C.A., Downey, J.R., Jr., Frurip, D.J., McDonald, R.A., & Syverd, A.N. (1985). JANAF thermodynamic tables, Journal of Physical and Chemical Reference Data, 14 (Supplement 1), 1–1856.
21. Liu, W., Vidic, R.D., & Brown, T.D. (1998) Optimization of sulfur impregnation protocol for fixed-bed application of activated carbon-based sorbents for gas-phase mercury removal, Environmental Science & Technology, 32, 531–538.
22. Lee, S.J., Seo, Y., Jurng, J., & Lee, T.G. Removal of gas-phase elemental mercury by iodine- and chlorine-impregnated activated carbons, Atmospheric Environment, 38, 4887–4893.
23. Miller, S.J., Dunham, G.E., Olson, E.S., & Brown, T.D. (2000). Flue gas effects on a carbon-based mercury sorbent. Fuel Processing Technology, 65/66, 343–363.
24. Olson, E.S., Laumb, J.D., Benson, S.A., Dunham, G.E., Sharma, R.K., Mibeck, B.A., Miller, S.J., Holmes, M.J., & Pavlish, J.H. (2003). An improved model for flue gas-mercury interactions on activated carbons, Proceedings of mega symposium and air & waste management association's specialty conference, Washington, DC.
25. Laumb, J.D., Benson, S.A., & Olson, E.S.X. (2004). X-ray photoelectron spectroscopy analysis of mer-

cury sorbent surface chemistry, Fuel Processing Technology, 85, 577–585.
26. Olson, E.S., Crocker, C.C., Benson, S.A., Pavlish, J.H., & Holmes, M.J.J. (2005). Surface compositions of carbon sorbents exposed to simulated low-rank coal flue gases, Air & Waste Management Association, 55, 747–754.
27. Carey, T.R., Hargrove, O.W., Richardson, C.F., Chang, R., & Meserole, F.B.J. (1998). Factors affecting mercury control in utility flue gas using activated carbon, Journal of the Air & Waste Management Association, 48, 1166.
28. Li, Y.H., Lee, C.W., & Gullett, B.K. (2002). The effect of activated carbon surface moisture on low temperature mercury adsorption, Carbon, 40, 65–72.
29. Lee, S., & Park, Y. (2003). Gas phase mercury removal by carbon-based sorbents, Fuel Processing Technology, 84, 197–206.
30. Li, Y.H., Lee, C.W., & Gullett, B.K. (2003). Importance of activated carbon's oxygen functional groups on elemental mercury adsorption, Fuel, 82, 451–457.
31. Chen, N., & Yang, R.T. (1998). Ab initio molecular orbital calculation on graphite: Selection of molecular system and model chemistry, Carbon, 36, 1061–1070.
32. Chen, N., & Yang, R.T. (1998) Ab initio molecular orbital study of the unified mechanism and pathways for gas-carbon reactions, Journal of Chemical Physics A, 102, 6348–6356.
33. Lamoen, D., & Persson, B.N.J. (1998). Adsorption of potassium and oxygen on graphite: A theoretical study, Journal of Chemical Physics, 108, 3332–3341.
34. Zhu, Z.H., & Lu, G.Q. (2004). Comparative study of Li, Na, and K adsorptions on graphite by using ab initio method, Langmuir, 20, 10751–10755.
35. Janiak, C., Hoffmann, Rr., Sjovall, P., & Kasemo, B. The potassium promoter function in the oxidation of graphite: An experimental and theoretical study, Langmuir, 9, 3427–3440.
36. Ohta, Y., & Ohta, K. (2005). First principle study of adsorption of atomic hydrogen on cluster-model surfaces, Synthetic Metals, 152, 329–332.
37. Pliego, J.R., Resende, S.M., & Humeres, E. (2005) Chemisorption of SO_2 on graphite surface: A theoretical ab initio and ideal lattice gas model study, Journal of Chemical Physics, 314, 127–133.
38. Collignon, B., Hoang, P.N.M., Picaud, S., & Rayez, J.C. (2005). Ab initio study of the water adsorption on hydroxylated graphite surfaces, Chemical Physics Letters, 406, 430–435.
39. Steckel, J.A. Ab initio modeling of neutral and cationic Hg-benzene complexes, Chemical Physics Letters, 409, 322–330.
40. Frisch, M.J., Trucks, G.W., Schlegel, H.B., Scuseria, G.E., Robb, M.A., Cheeseman, J.R., Montgomery, J.A., Jr., Vreven, T., Kudin, K.N., Burant, J.C., Millam, J.M., Iyengar, S.S., Tomasi, J., Barone, V., Mennucci, B., Cossi, M., Scalmani, G., Rega, N., Petersson, G.A., Nakatsuji, H., Hada, M., Ehara, M., Toyota, K., Fukuda, R., Hasegawa, J., Ishida, M., Nakajima, T., Honda, Y., Kitao, O., Nakai, H., Klene, M., Li, X., Knox, J.E., Hratchian, H.P., Cross, J.B., Adamo, C., Jaramillo, J., Gomperts, R., Stratmann, R.E., Yazyev, O., Austin, A.J., Cammi, R., Pomelli, C., Ochterski, J.W., Ayala, P.Y., Morokuma, K., Voth, G.A., Salvador, P., Dannenberg, J.J., Zakrzewski, V.G., Dapprich, S., Daniels, A.D., Strain, M.C., Farkas, O., Malick, D.K., Rabuck, A.D., Raghavachari, K., Foresman, J.B., Ortiz, J.V., Cui, Q., Baboul, A.G., Clifford, S., Cioslowski, J., Stefanov, B.B., Liu, G., Liashenko, A., Piskorz, P., Komaromi, I., Martin, R.L., Fox, D.J., Keith, T., Al-Laham, M.A., Peng, C.Y., Nanayakkara, A., Challacombe, M., Gill, P.M.W., Johnson, B., Chen, W., Wong, M.W., Gonzalez, C., & Pople, J.A. (2003). Gaussian 03, Revision B. 04, Gaussian, Inc., Pittsburgh PA.
41. Hay, P.J., & Wadt, W.R. (1985). Ab initio effective core potentials for molecular calculations. Potentials for the transition metal atoms Sc to Hg, Journal of Chemical Physics, 82, 270–283.
42. Hay, P.J., & Wadt, W.R. (1985). Ab initio effective core potentials for molecular calculations. Potentials for K to Au including outermost core orbitals, Journal of Chemical Physics, 82, 299–310.
43. Wadt, W.R., & Hay, P.J. (1985). Ab initio effective core potentials for molecular calculations. Potentials for main group elements Na to Bi, Journal of Chemical Physics, 82, 284–298.
44. Morimoto, T., Wu, S., Uddin, M.A., & Sasaoka, E. (2005). Characteristics of the mercury vapor removal from coal combustion flue gas by activated carbon using H_2S, Fuel, 84, 1968–1974.